

## Supporting Information

### Indolocarbazole-core linked triphenylamine as an interfacial passivation layer for perovskite solar cells

Yulin Tan <sup>a</sup>, Haoliang Cheng <sup>a</sup>, Yang Zhao <sup>a</sup>, Li Wan <sup>a</sup>, Zhong-Sheng Wang\*<sup>a</sup>

Department of Chemistry, Shanghai Key Laboratory of Molecular Catalysis and Innovative Materials, Laboratory of Advanced Materials, iChEM (Collaborative Innovation Center of Chemistry for Energy Materials), Fudan University, 2205 Songhu Road, Shanghai 200438, China

#### Materials

N, N-dimethylformide (DMF), acetonitrile, dichloromethane (DCM), toluene, isopropanol, chloroform and ethanol were obtained from commercial sources and used without further purification. 1H-indole, 4-bromobenzaldehyde, 1-iodo-4-methoxybenzene, 4-methoxyaniline, (4-iodophenyl)(methyl)sulfane, 4-(methylthio)aniline, hydriodic acid, tris(dibenzylideneacetone)dipalladium (Pd<sub>2</sub>(dba)<sub>3</sub>), palladium acetate (Pd(AcO)<sub>2</sub>), tri-tert-butylphosphine (P(t-Bu)<sub>3</sub>), potassium tert-butoxide (t-BuOK), sodium tert-butoxide (t-BuONa) and 2-dicyclohexylphosphino-2',4',6'-triisopropylbiphenyl (XPhos) were purchased from J&K Scientific (China). 4-tert-butylpyridine (TBP) and lithium bis-(trifluoromethanesulfonyl) imide (LiTFSI), methylammonium iodide (MAI, 99.5%), lead iodide (PbI<sub>2</sub>, 99.9985%) and Spiro-OMeTAD were purchased from Xi'an Polymer Light Technology Corp (China).

#### Experimental section

**Device fabrication:** We use detergent, deionized water, acetone, and isopropanol (IPA) to clean the glass/ITO substrates by successive sonication for 20 min each, and

then dry them with a high-speed nitrogen stream. Treat the cleaned glass/ITO with oxygen plasma at 120 °C for 20 min before use. SnO<sub>2</sub> quantum dots (synthesized according to previously reported literature<sup>1</sup>) are spin-coated onto ITO substrates with 1000 rpm for 3 s and 3000 rpm for 30 s successively, and then annealed in ambient conditions at 200 °C for 60 min. The prepared SnO<sub>2</sub> layer needs to be treated with oxygen plasma for another 20 min before spin-coating the perovskite layer. For MAPbI<sub>3</sub> layer, 1.3M PbI<sub>2</sub> and 1.3M MAI are dissolved in DMSO/DMF (v/v=1:4) mixture solution, and stirred at 70 °C for 4 h in a glovebox to prepare a precursor solution. Use a one-step method to spin-coat the perovskite precursor solution onto SnO<sub>2</sub> layer at 1000 rpm for 3 s and 5000 rpm for 30 s, at 10 s after the start of spin-coating, pour 300 μL of chlorobenzene solvent onto the substrate. Subsequently, the perovskite layer is thermally annealed at 70 °C for 30 s, and then 100 °C for 10 min through a two-step process. For the TM5 (or TM6)-coated perovskite layer, chlorobenzene solutions loaded with different concentrations of TM5 (or TM6) are spin-coated on the prepared perovskite layer at 3000 rpm for 30 s. For TM5 (or TM6) as HTL, 10 mg cm<sup>-3</sup> of chlorobenzene solution of TM5 (or TM6) is spin-coated on the prepared perovskite film at 2000 rpm for 30 s. For doped Spiro-OMeTAD as HTL, Spiro-OMeTAD [72.3 mg Spiro-OMeTAD in 1 cm<sup>3</sup> chlorobenzene with 28.8 μL TBP and 17.5 μL Li-TFSI stock solution (520 mg Li-TFSI in 1 cm<sup>3</sup> acetonitrile)] is spin-coated on the perovskite film at 3000 rpm for 30 s. Finally, 80 nm Au is thermally evaporated onto the substrate as metal electrode in a vacuum chamber at a base pressure of 3×10<sup>-4</sup> mbar and a rate of 0.5 Å/s to complete the fabrication process.

**Device characterization:**  $^1\text{H}$  NMR and  $^{13}\text{C}$  NMR spectra are recorded on a Bruker AM-400 spectrometer. The reported chemical shifts are against TMS. High Resolution Mass Spectroscopy (HRMS) are obtained with a Micromass GCT-TOF mass spectrometer. Cyclic voltammetry (CV) measurements of the TM5 or TM6 molecules in dichloromethane with 0.1 M TBAPF<sub>6</sub> as the supporting electrolyte are performed on an electrochemistry workstation (CHI660C Instruments, Shanghai Chenhua Instrument Corp., China). An Ag/AgNO<sub>3</sub> electrode is used as the reference electrode, a carbon-glass electrode as the working electrode, a Pt electrode as the counter electrode and Spiro-OMeTAD as a reference. Differential scanning calorimetry (DSC) and thermogravimetric analysis (TGA) measurements are carried out on a synchronous thermal analyzer (SDT Q600, America TA). The photoluminescence (PL) spectra are measured using a spectrofluorophotometer (RF-5301PC, Shimadzu) with a monochromatic light S-4 (500 nm) from a xenon lamp source. Fourier transform infrared (FTIR) measurements are performed on Shimadzu IRAffinity-1 FTIR spectrometer with a resolution of 2 cm<sup>-1</sup>. Scanning electron microscopy (SEM) (S4800, Hitachi, Japan) is used to obtain the SEM images. The perovskite crystal structure is investigated in the range of 5 to 50° in  $\theta$  to  $2\theta$  mode using a Bruker D8 Advance X-ray diffractometer (Cu K $\alpha$ 1,  $\lambda = 0.154$  nm; 40 kV, 40 mA). X-ray photoelectron spectroscopy (XPS) measurements were carried out on Axis Ultra D1d with monochromatic AlK $\alpha$  radiation (1486.6 eV) (40 W, 200 mm spot size, 0.1 eV resolution). The electrochemical impedance spectroscopy (EIS) measurement is conducted with the Zahner IM6 system. Current-voltage ( $J$ - $V$ )

characteristics are performed under 1-sun (AM 1.5G) illumination with a computer-controlled Keithley 2420 source meter and Newport-94043A solar simulator (400 W). A National Renewable Energy Laboratory calibrated silicon photodiode is used to calibrate the solar simulator's light intensity. External quantum efficiency (EQE) measurements for perovskite solar cells (PSCs) are conducted on a SM-250 hyper mono-light system (Bunkoukeiki, Japan). Contact angles are measured on Dataphysics-OCA20 (Dataphysics, Germany). Mott-Schottky measurements were carried out in the dark with an electrochemistry workstation (CHI660C Instruments, Shanghai Chenhua Instrument Corp., Shanghai, China). The open-circuit voltage decay (OCVD) was recorded by electrochemical workstation (Zahner, Germany) with Newport-94043A solar simulator supplied 100 mW cm<sup>-2</sup> light intensity to excite the perovskite solar cells. The atomic force microscopy (AFM) images were observed on the Dimension 3100 V AFM with tapping mode (Veeco, USA).

## Equations

$$J_D = \frac{9\varepsilon\varepsilon_0\mu V_b^2}{8L^3} \quad (\text{S1})$$

$J_D$  is current density,  $\varepsilon$  is relative permittivity (3 for organic molecules),<sup>2</sup>  $\varepsilon_0$  is vacuum dielectric constant,  $V_b$  is applied voltage,  $L$  is thickness of the organic molecular layer (about 20 nm) in eq S1.

$$N_t = \frac{2\varepsilon_r\varepsilon_0}{eL^2} \cdot V_{\text{TFL}} \quad (\text{S2})$$

$\varepsilon_r$  is the relative dielectric constant of the perovskite film (MAPbI<sub>3</sub> is 32).<sup>2</sup>  $\varepsilon_0$  is the vacuum dielectric constant,  $e$  is the elementary charge, and  $L$  is the thickness of the perovskite film (~300 nm, see Fig. S15) in eq S2.

$$I(t) = A_1 \exp\left(-\frac{t}{\tau_1}\right) + A_2 \exp\left(-\frac{t}{\tau_2}\right) \quad (\text{S3})$$

$$\tau_{\text{ave}} = A_1 \tau_1 + A_2 \tau_2 \quad (\text{S4})$$

$\tau_1$  is the fast decay time constant, and  $\tau_2$  is the slow decay time constant.  $A_1$  and  $A_2$  are the fractional intensities,  $\tau_{\text{ave}}$  is the average carrier lifetime, in eq S3 and S4.

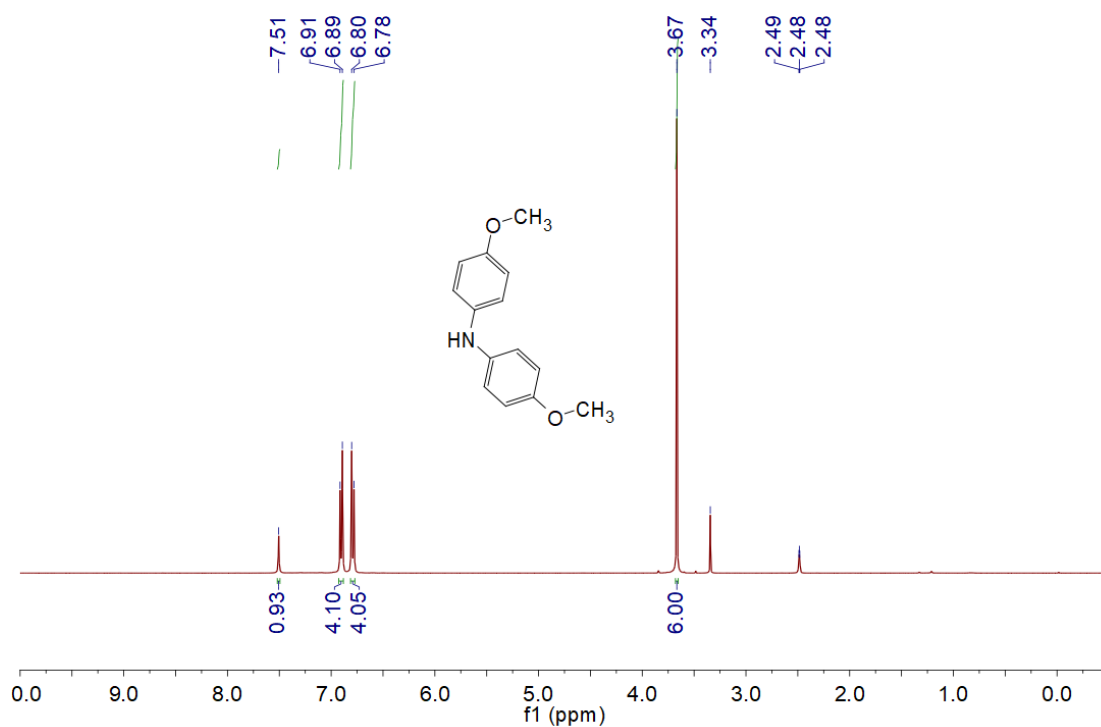
$$V_{\text{oc}} = \frac{nKT \ln(J)}{e} + C \quad (\text{S5})$$

$n$  is the ideal factor,  $T$  is the absolute temperature, and  $C$  is a constant in eq S5.

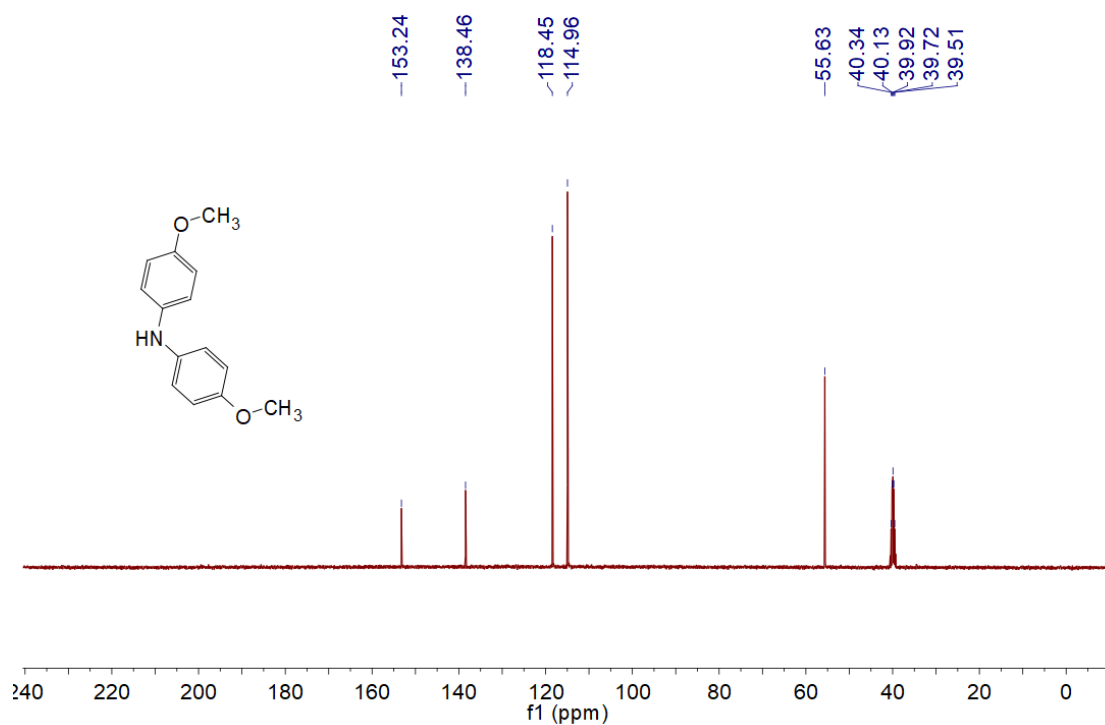
$$\frac{1}{C^2} = \frac{2}{\epsilon \epsilon_0 e A^2 N_d} (V_{bi} - V) \quad (\text{S6})$$

$C$  represents the capacitance,  $A$  is the effective area,  $V$  is the applied bias voltage,  $e$  is the elementary charge,  $N_d$  is the carrier density,  $\epsilon_0$  is the vacuum permittivity,  $\epsilon$  is the relative dielectric constant in eq S6.

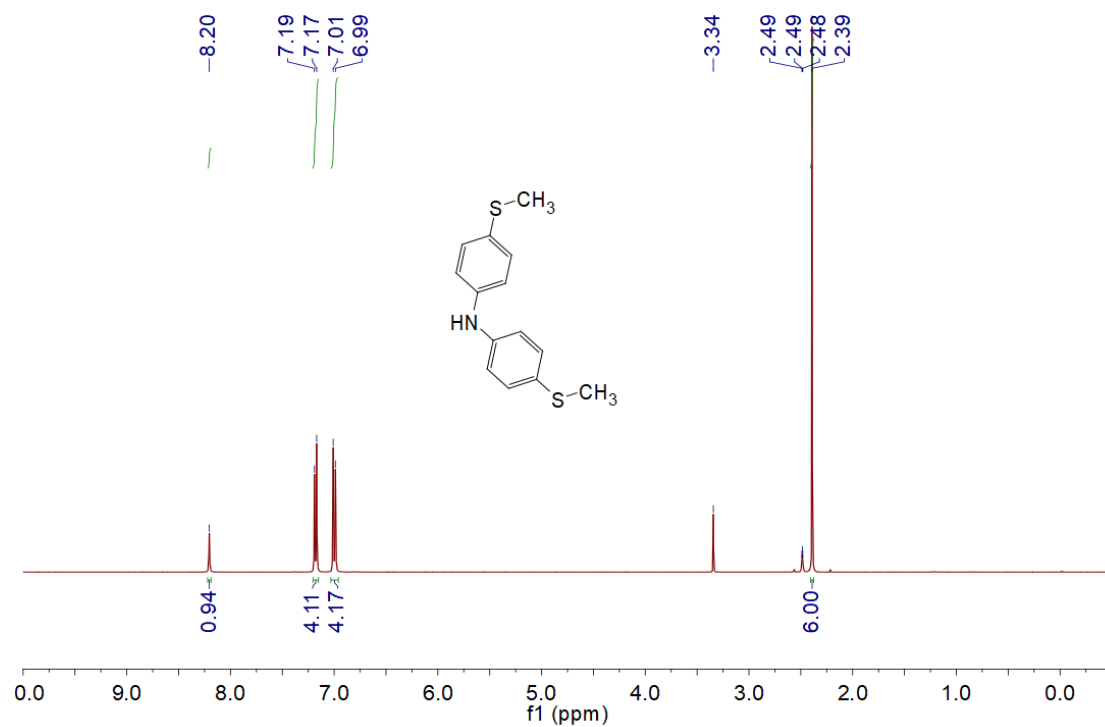
### Supporting figures



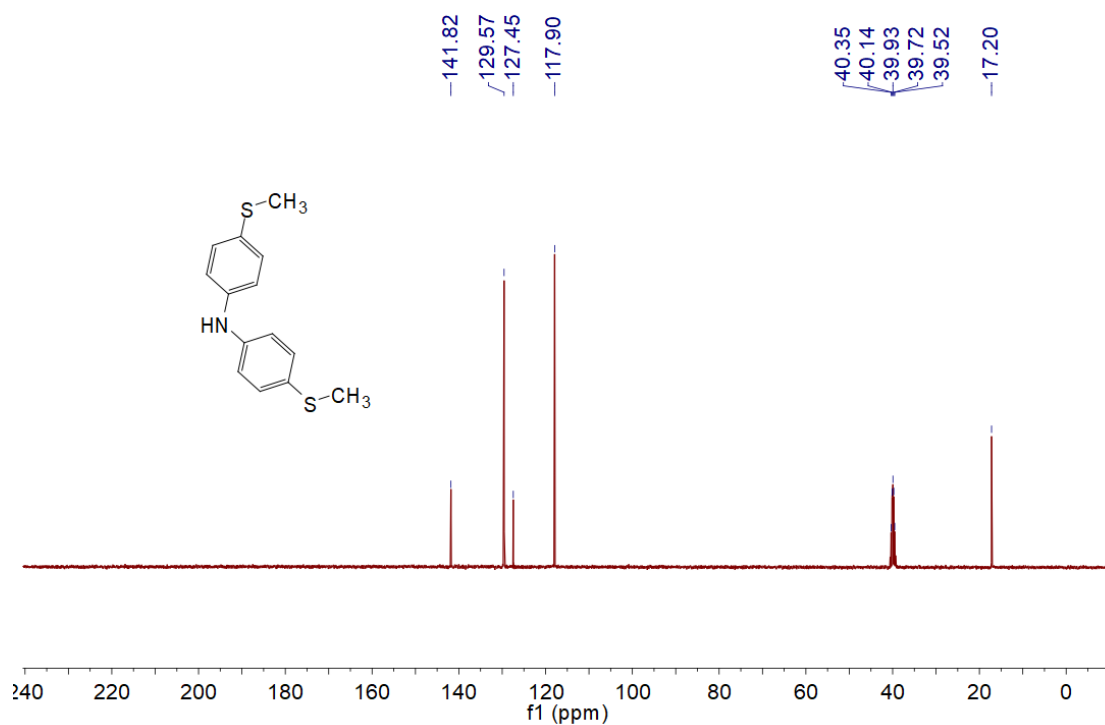
**Fig. S1.**  $^1\text{H}$  NMR spectrum (400 MHz, DMSO- $d_6$ ) of compound 3: 7.51 (s, 2H), 6.90 (d,  $J = 8.0$  Hz, 4H), 6.79 (d,  $J = 8.0$  Hz, 4H), 3.67 (s, 6H).



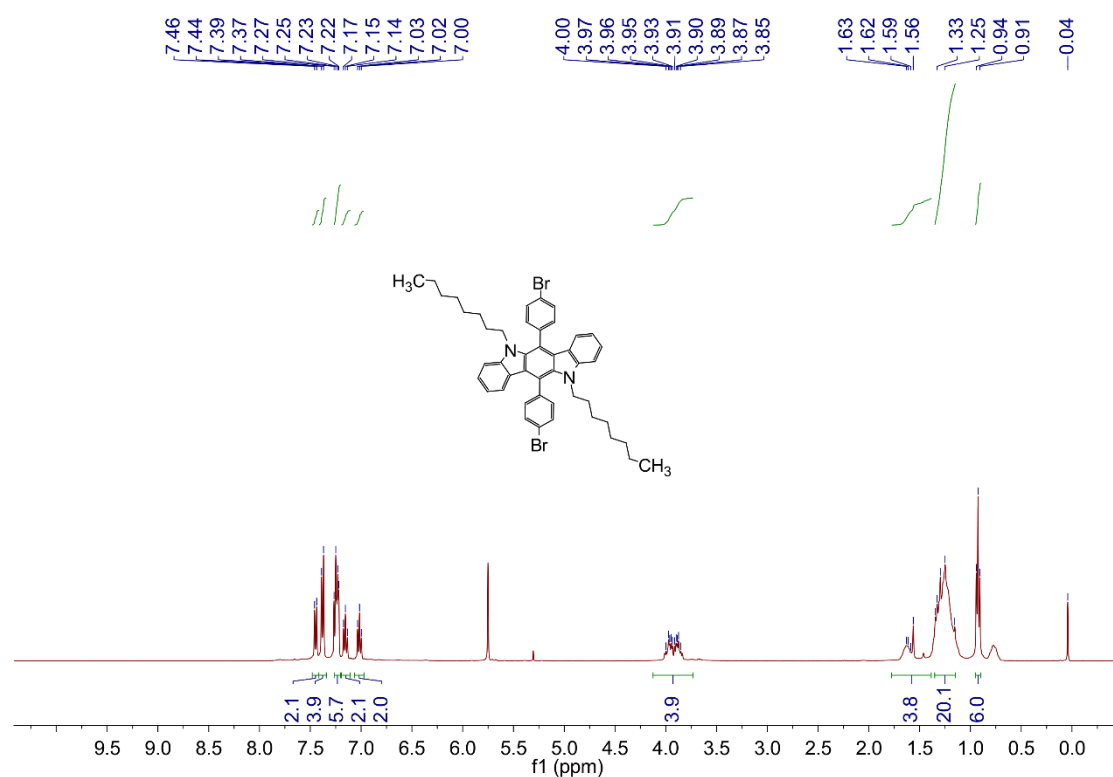
**Fig. S2.**  $^{13}\text{C}$  NMR spectrum (101 MHz, DMSO- $d_6$ ) of compound 3: 153.2, 138.5, 118.5, 115.0, 55.6.



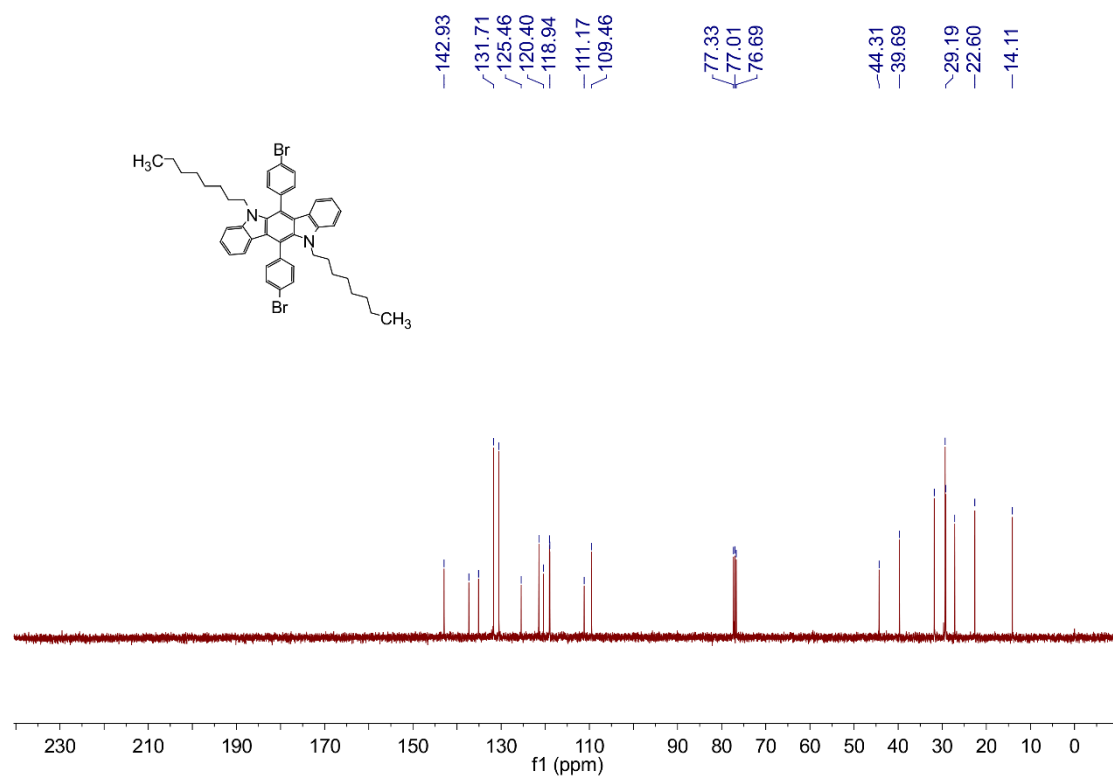
**Fig. S3.**  $^1\text{H}$  NMR spectrum (400 MHz, DMSO- $d_6$ ) of compound 6: 8.20 (s, 2H), 7.18 (d,  $J = 8.0$  Hz, 4H), 7.00 (d,  $J = 8.0$  Hz, 4H), 2.39 (s, 6H).



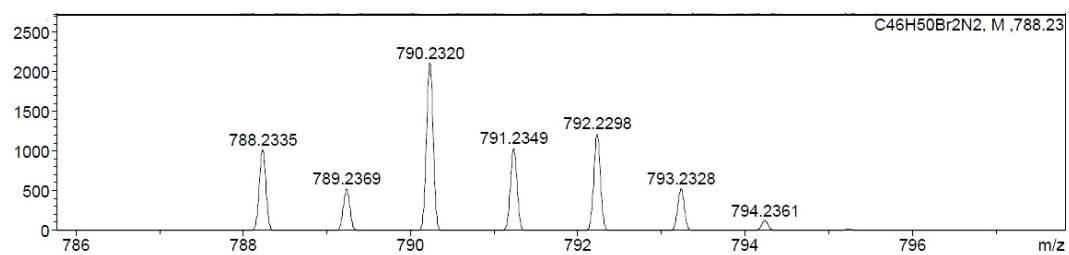
**Fig. S4.**  $^{13}\text{C}$  NMR spectrum (101 MHz, DMSO- $d_6$ ) of compound 6: 141.8, 129.6, 127.5, 117.9, 17.2.



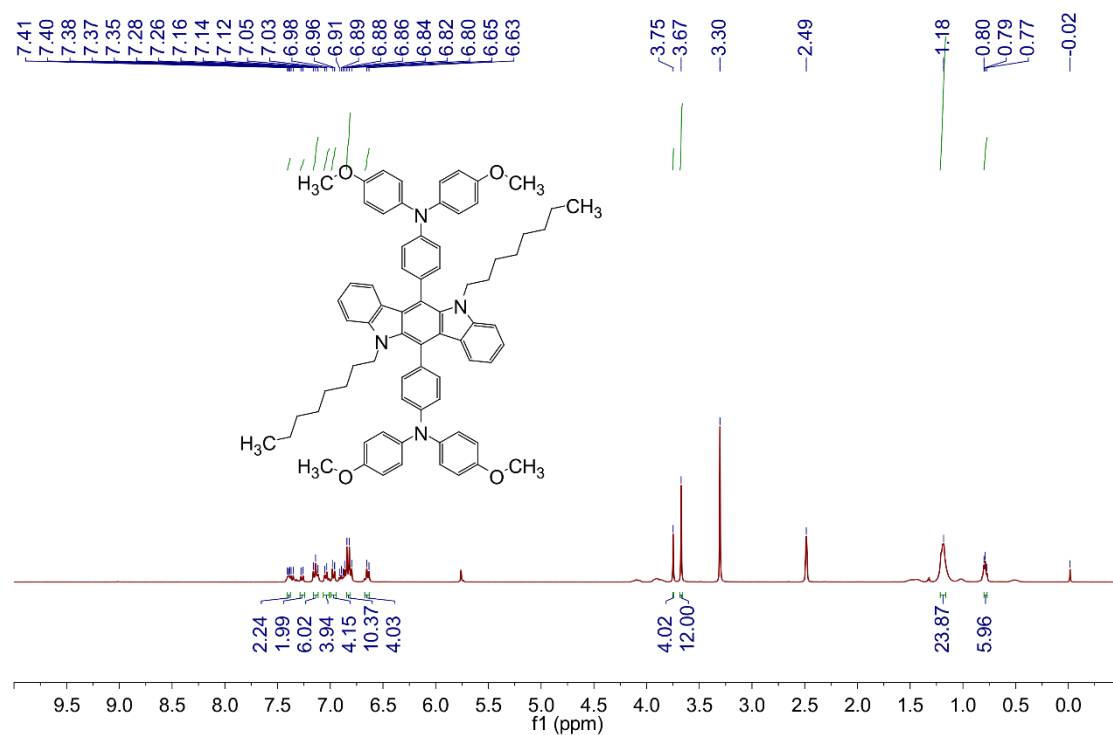
**Fig. S5.**  $^1\text{H}$  NMR spectrum of compound 10.



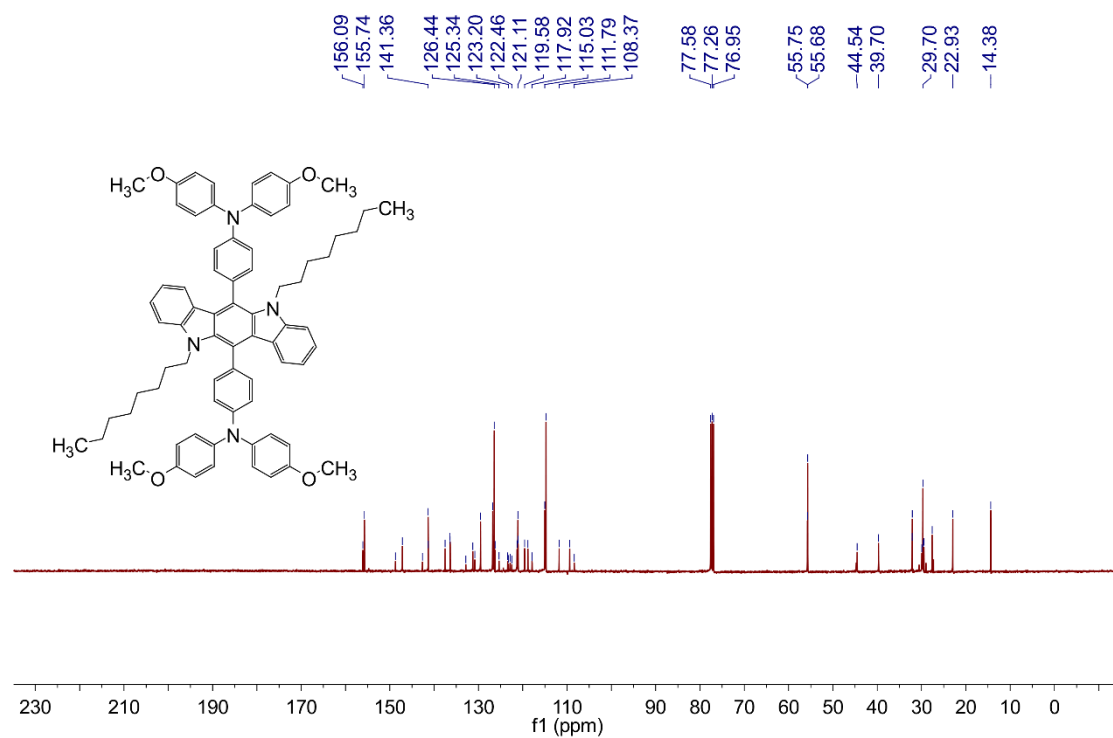
**Fig. S6.**  $^{13}\text{C}$  NMR spectrum of compound 10.



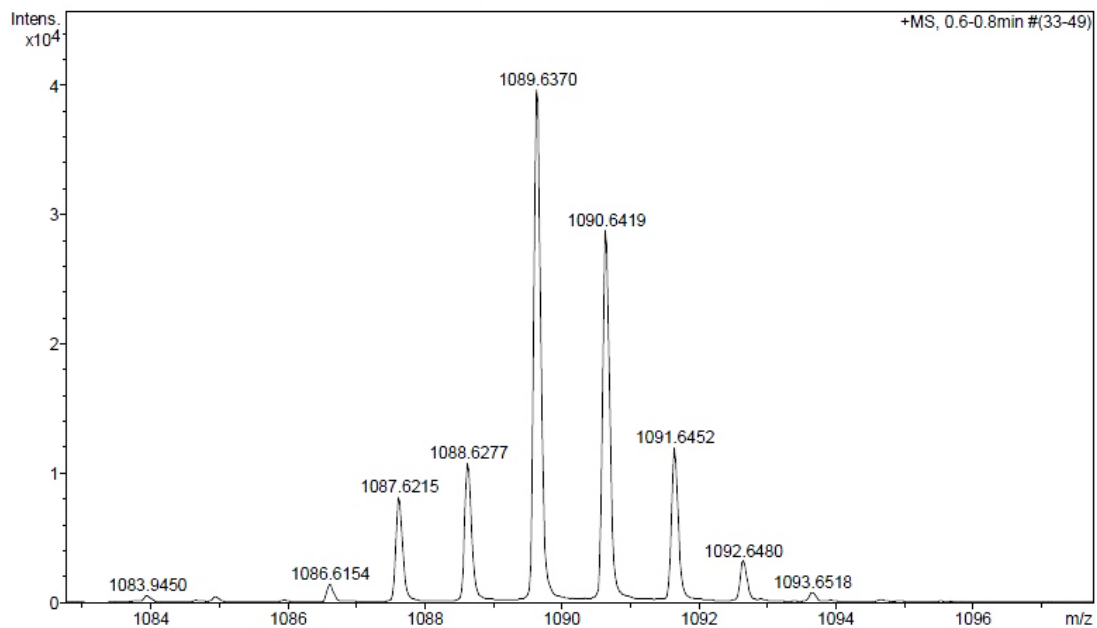
**Fig. S7.** ESI-HRMS spectrum of compound 10



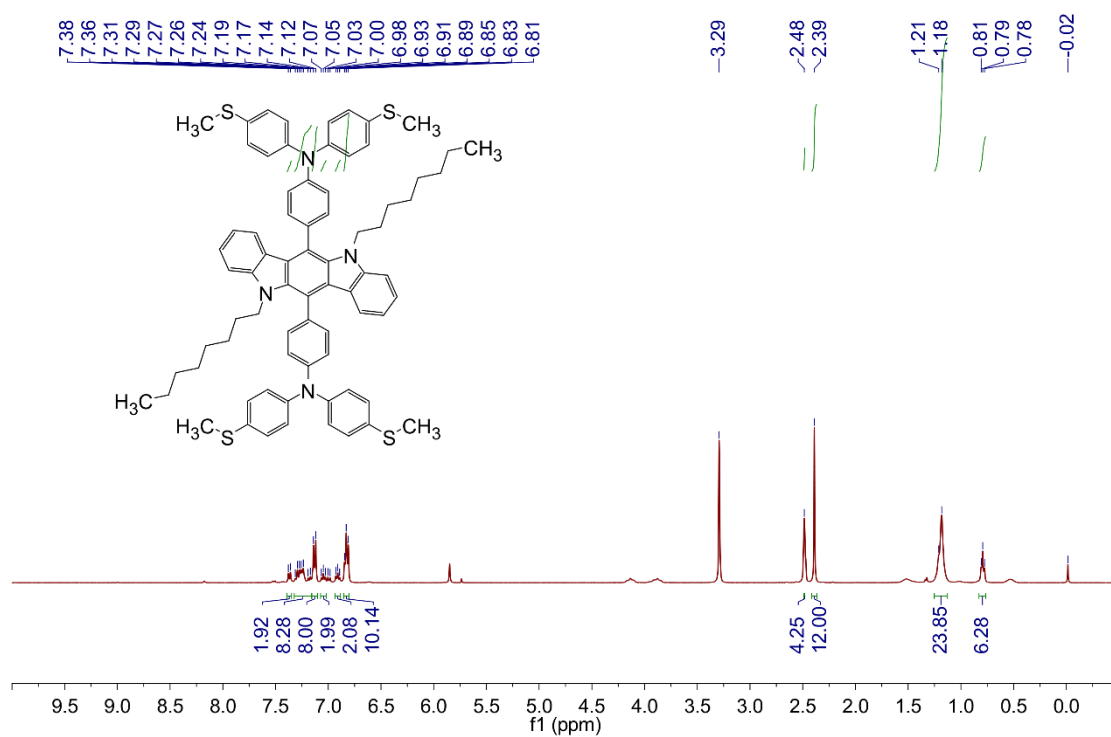
**Fig. S8.** <sup>1</sup>H NMR spectrum of TM5.



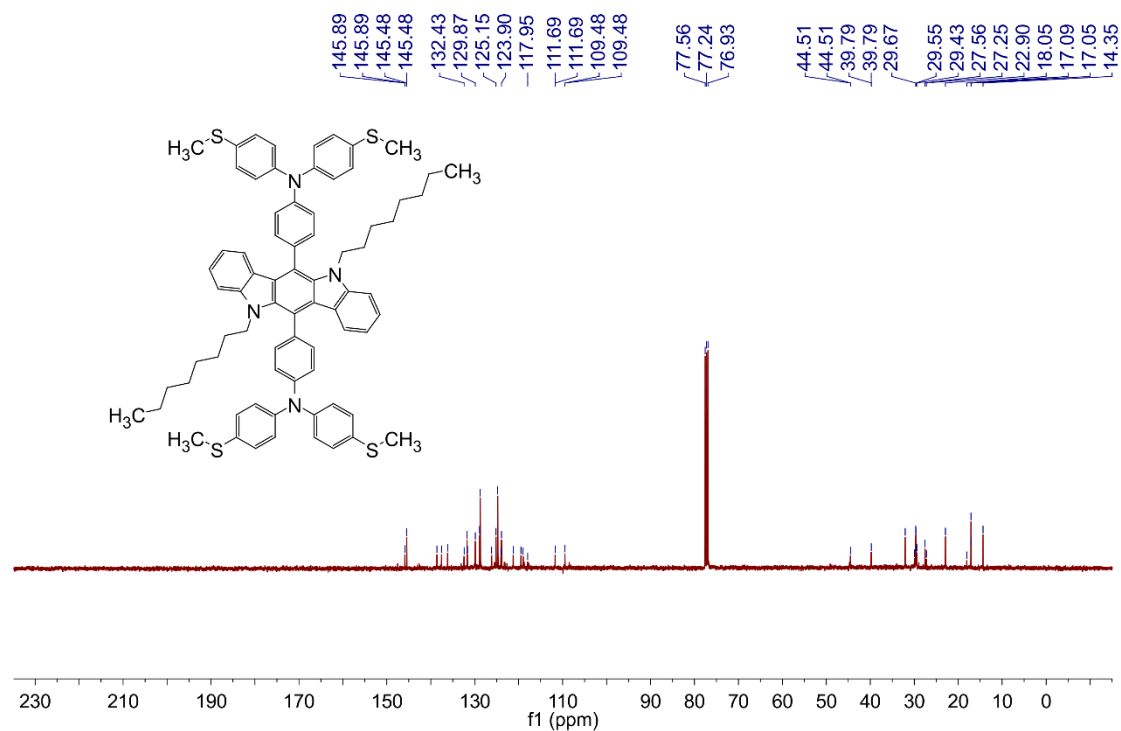
**Fig. S9.** <sup>13</sup>C NMR spectrum of TM5.



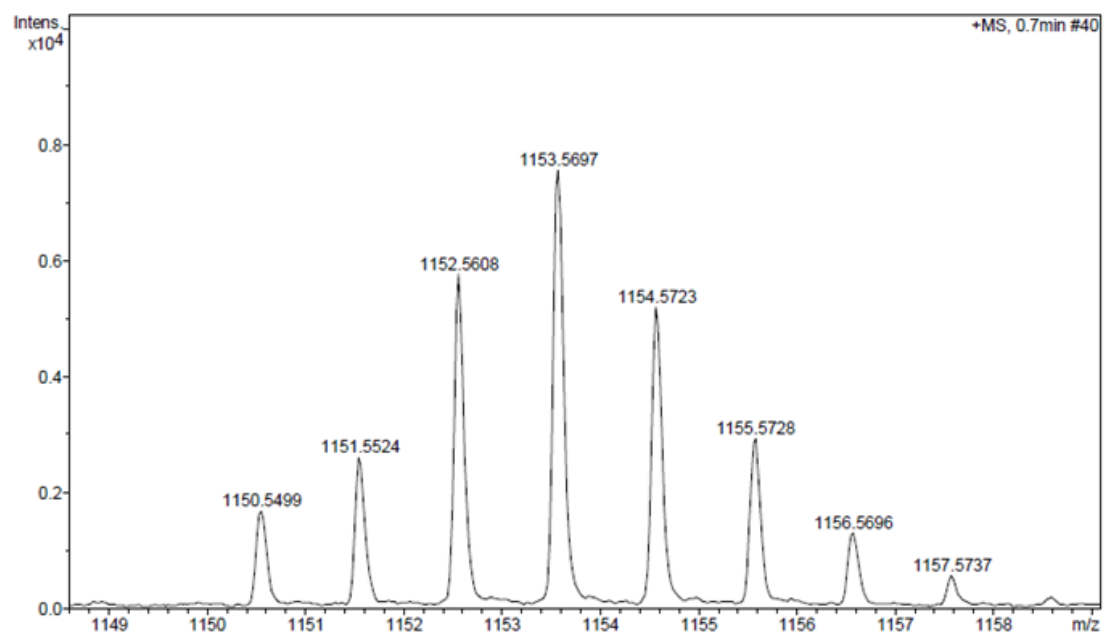
**Fig. S10.** ESI-HRMS spectrum of TM5.



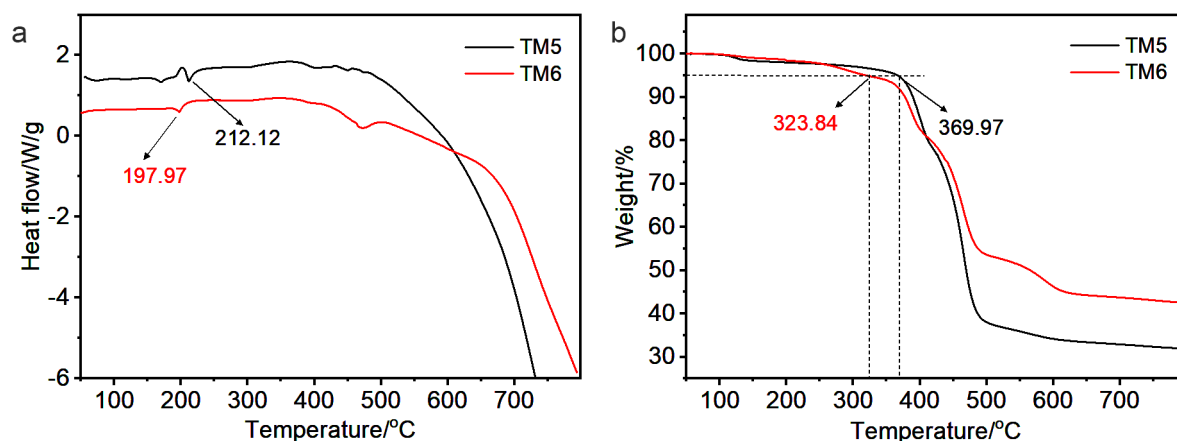
**Fig. S11.**  $^1\text{H}$  NMR spectrum of TM6.



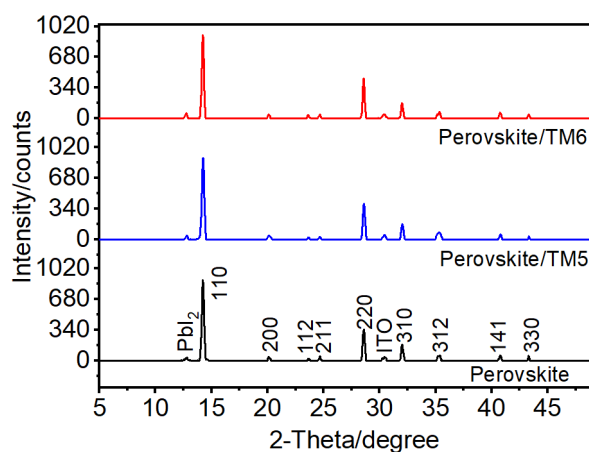
**Fig. S12.**  $^{13}\text{C}$  NMR spectrum of TM6.



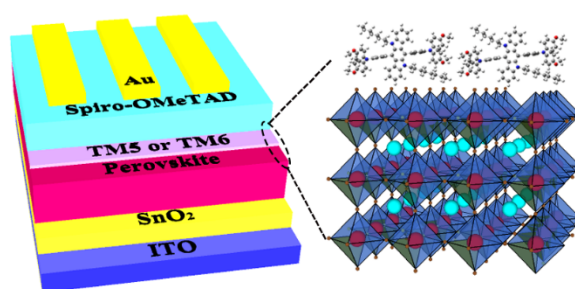
**Fig. S13.** ESI-HRMS spectrum of TM6.



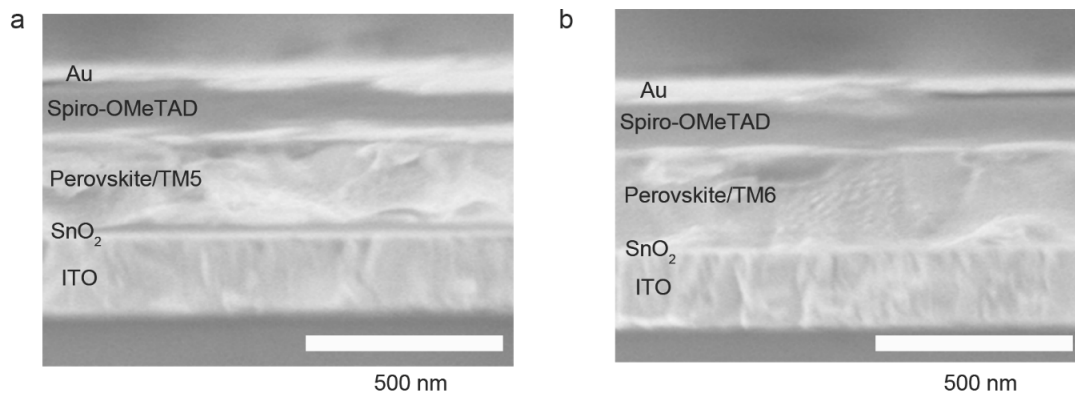
**Fig. S14.** (a) DSC and (b) TGA curves of TM5 and TM6.



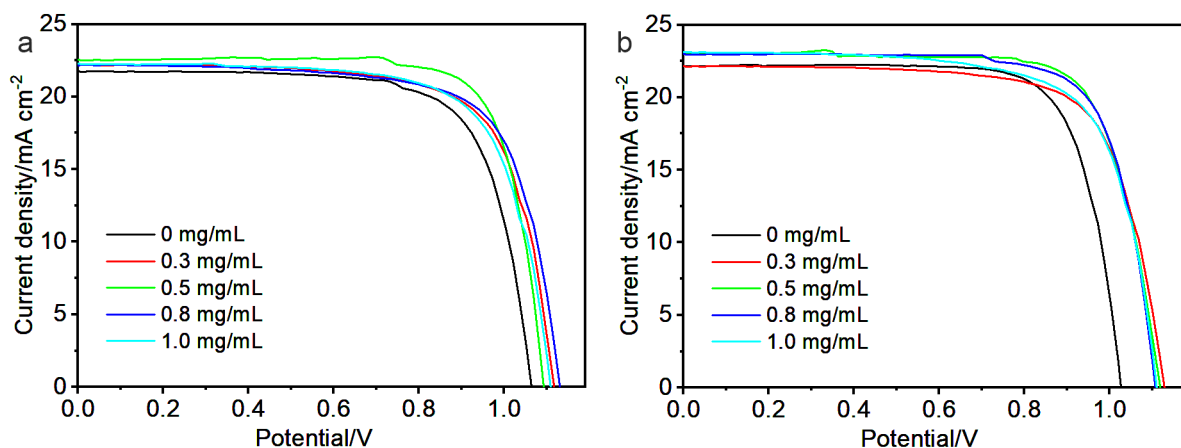
**Fig. S15.** XRD patterns of the pristine, TM5-coated and TM6-coated perovskite films.



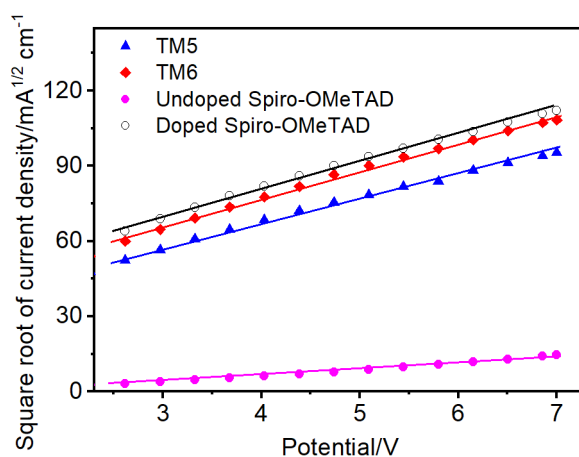
**Fig. S16.** n-i-p planar structure of PSCs: ITO/SnO<sub>2</sub>/MAPbI<sub>3</sub>/TM5 (or TM6)/Spiro-OMeTAD/Au.



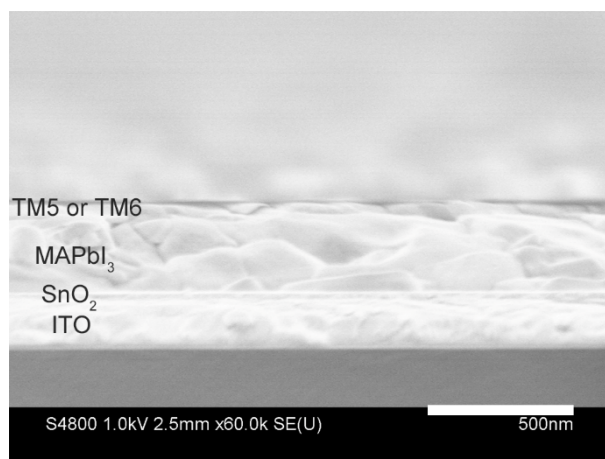
**Fig. S17.** Cross-sectional SEM images of the (a) TM5- and (b) TM6-coated PSCs.



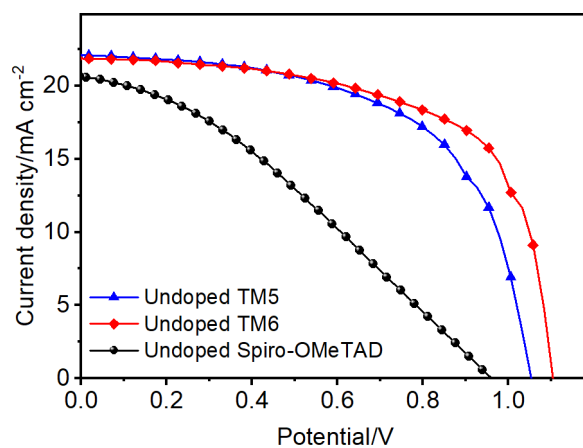
**Fig. S18.** The  $J$ - $V$  characteristics of the PSCs with different concentrations: (a) TM5 and (b) TM6.



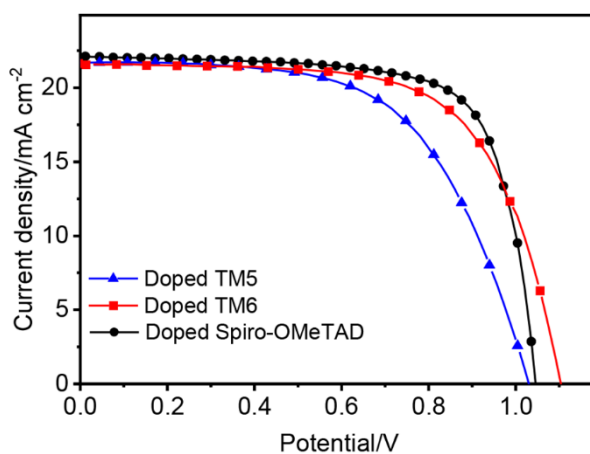
**Fig. S19.** SCLC mobility of devices with the structure of ITO/PEDOT:PSS/TM5 (or TM6)/MoO<sub>3</sub>/Ag, ITO/PEDOT:PSS/undoped Spiro-OMeTAD/MoO<sub>3</sub>/Ag and ITO/PEDOT:PSS/doped Spiro-OMeTAD/MoO<sub>3</sub>/Ag in the dark.



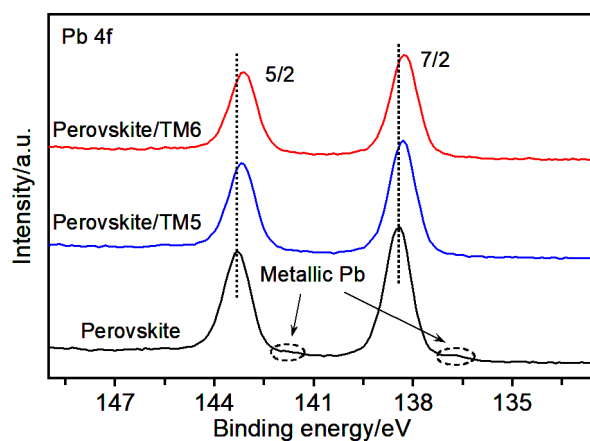
**Fig. S20.** The cross-sectional SEM image of the ITO/SnO<sub>2</sub>/MAPbI<sub>3</sub>/TM5 (or TM6) device.



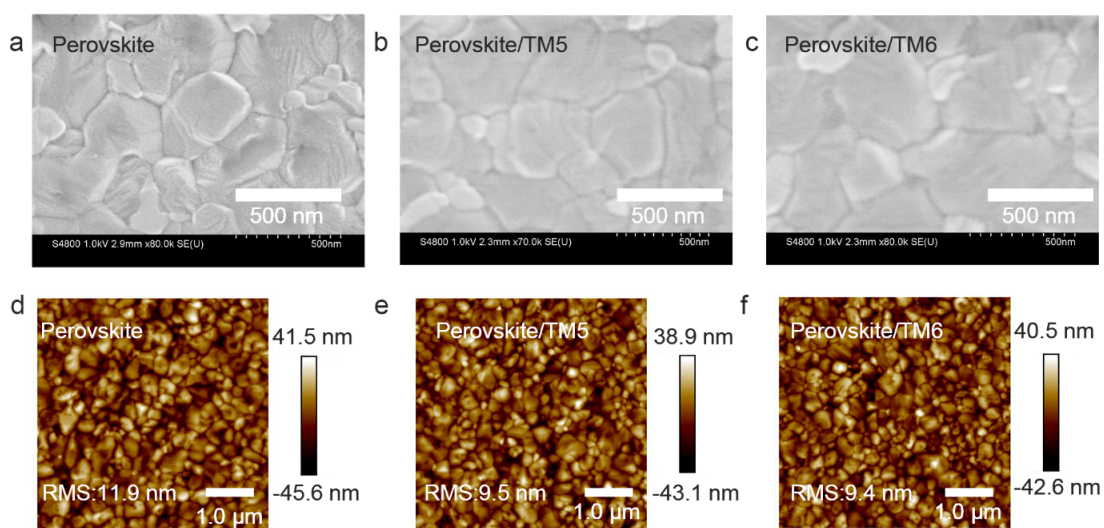
**Fig. S21.** *J-V* curves of PSCs with undoped HTLs.



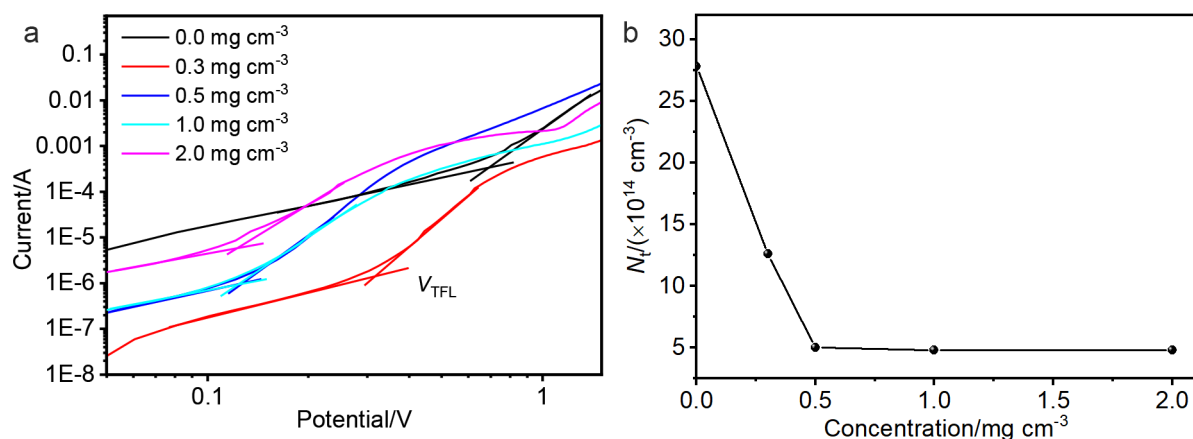
**Fig. S22.** *J-V* curves of PSCs with doped HTLs.



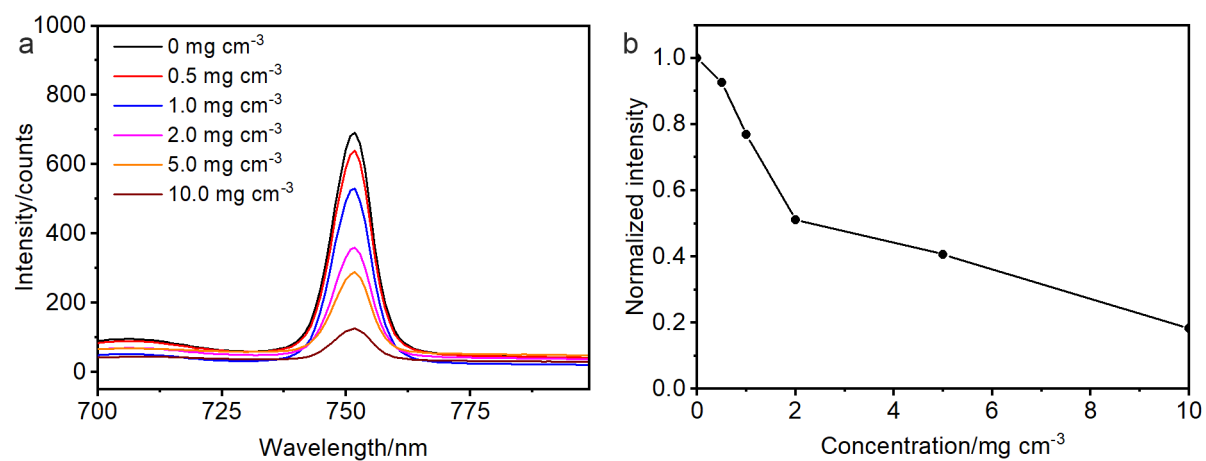
**Fig. S23.** XPS spectra of Pb 4f for the pristine, TM5- and TM6-coated perovskite films, respectively.



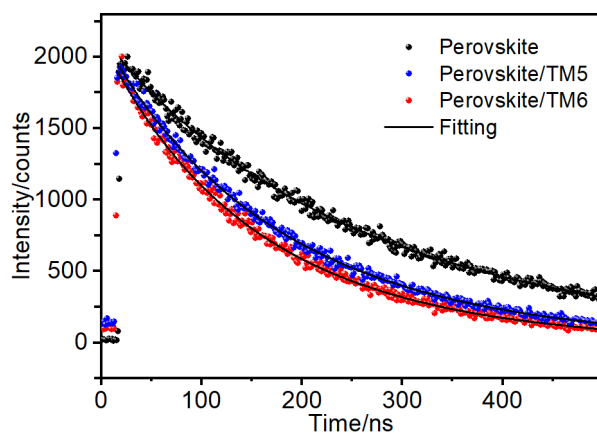
**Fig. S24.** Top-view SEM images of (a) the pristine perovskite film, (b) the TM5-coated perovskite film and (c) the TM6-coated perovskite film. AFM images ( $5 \times 5 \mu\text{m}$ ) of (d) the control, (e) the TM5-coated and (f) the TM6-coated perovskite films.



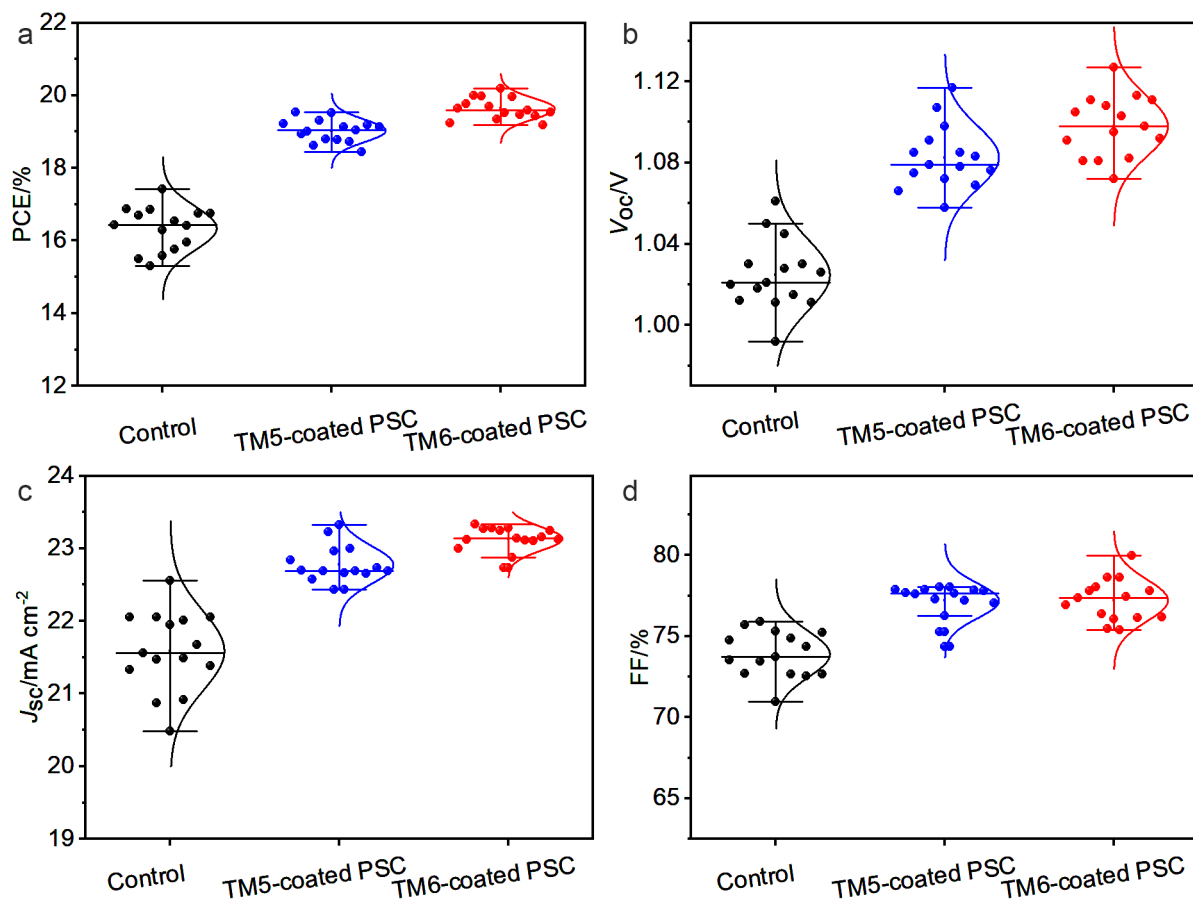
**Fig. S25.** (a) SCLC curves of TM6-based devices (ITO/SnO<sub>2</sub>/Perovskite/TM6/PCBM/Ag) with different concentrations of TM6. (b) The relationship between  $N_t$  against concentration of TM6 derived from the curves in (a).



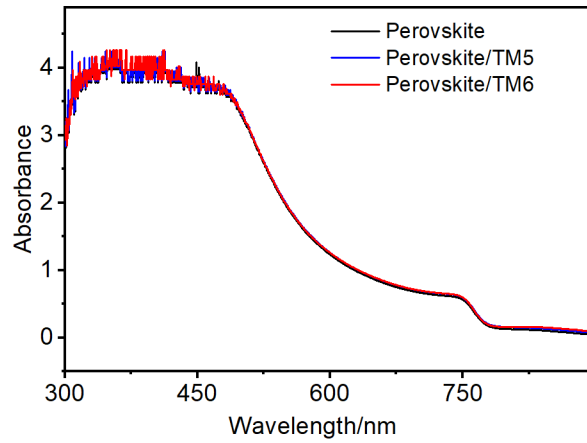
**Fig. 26.** (a) Steady-state PL spectra of the perovskite films with different concentrations of TM6. (b) The evolution of normalized PL intensity derived from (a) with the changes of the concentrations of TM6.



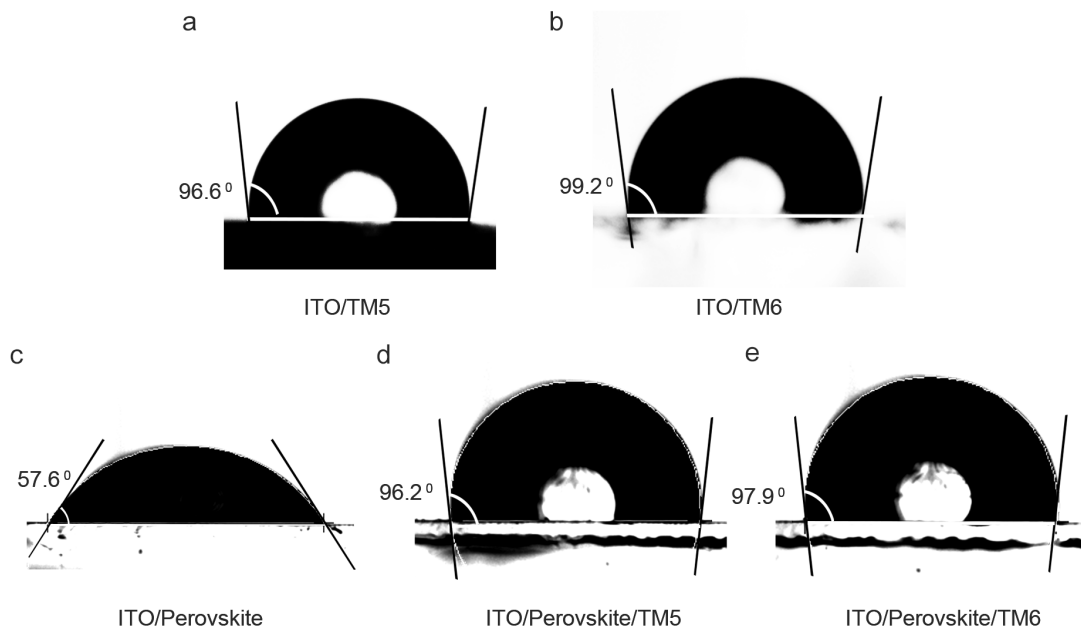
**Fig. S27.** TRPL spectra of the related perovskite films without HTL.



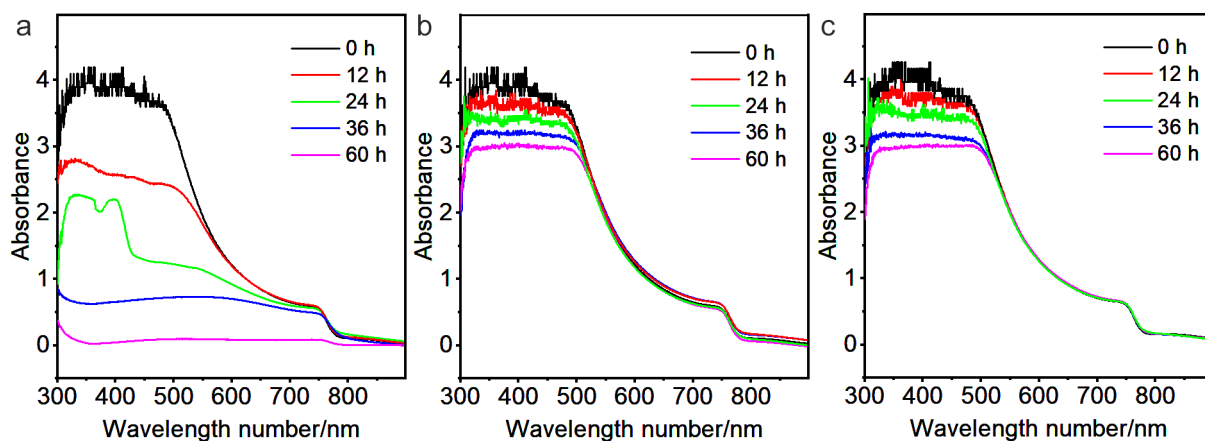
**Fig. S28.** Statistical plots of (a) PCE, (b)  $V_{oc}$ , (c)  $J_{sc}$ , and (d) FF of the relevant devices.



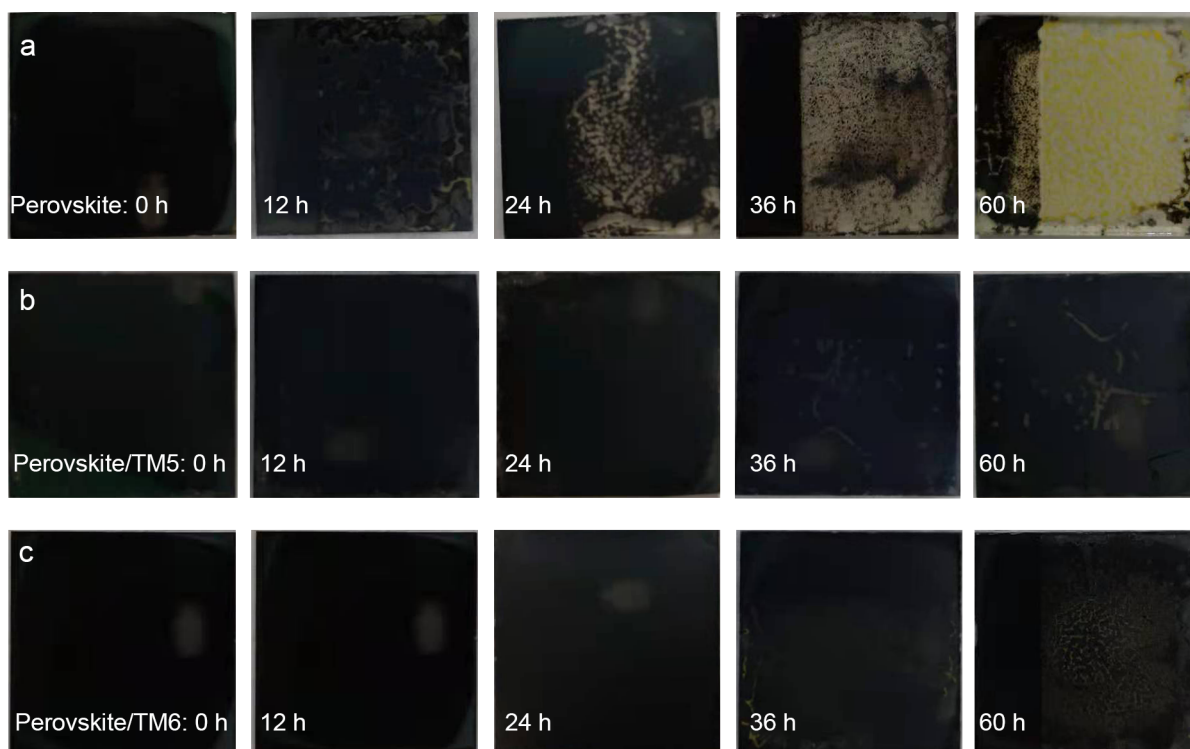
**Fig. S29.** UV-vis spectra of the control, TM5- and TM6-coated perovskite films.



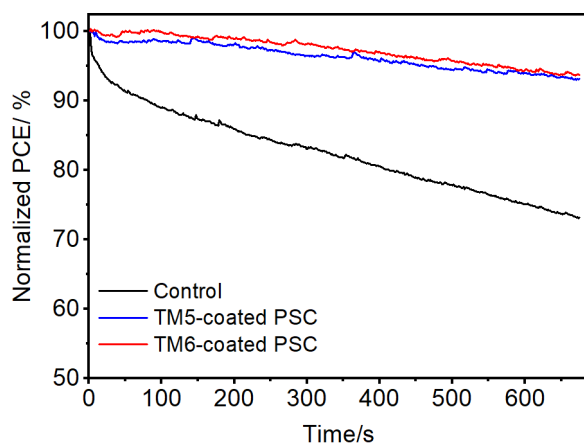
**Fig. S30.** Water contact angles on the surface of (a) the ITO/TM5 film, (b) the ITO/TM6 film, (c) the ITO/Perovskite film, (d) the ITO/Perovskite/TM5 film and (e) the ITO/Perovskite/TM6 film.



**Fig. S31.** Evolution of UV-vis spectra with time for perovskite films: (a) the pristine perovskite film, (b) the TM5-coated perovskite film and (c) the TM6-coated perovskite film.



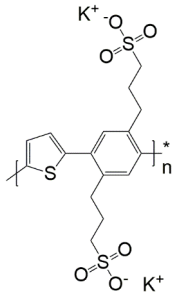
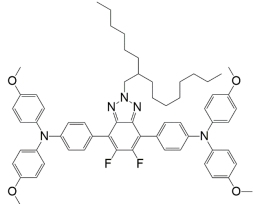
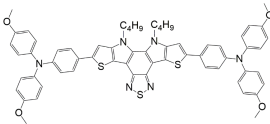
**Fig. S32.** The evolution of images for (a) the control, (b) TM5-coated and (c) TM6-coated perovskite films over time.



**Fig. S33.** The operational stability of PSCs under a constant illumination (AM1.5 G,  $100 \text{ mW cm}^{-2}$ ) at an ambient environment (20-30 °C and 85-90% RH). The devices are biased at their maximum power points of 0.82, 0.89 and 0.91 V for the control, TM5- and TM6-coated PSCs, respectively.

**Table S1.** Summary on passivation materials in the literature reports.

Name	Structure	Interactions	PCE/%	Ref
TFMBAI		F...H; 2D/3D	23.94	14
TPA-PEABr		2D	18.15	15
F8IC		S...Pb; C=O...Pb; F...H	18.40	10
SM2		IDTT...Pb	21.2	16
P-Si		N/A	21.5	17

TB(K)		K <sup>+</sup>	20.01	18
2FBTA-1		F---Pb; F---H	21.2	19
BDAD		S---Pb; N---Pb	22.76	20

**Table S2.** Photovoltaic performance of TM5-coated PSCs with different concentrations (*c*).

<i>c</i> /mg cm <sup>-3</sup>	<i>V</i> <sub>oc</sub> /V	<i>J</i> <sub>sc</sub> /mA cm <sup>-2</sup>	FF/%	PCE/%
0	1.064	21.74	72.52	16.77
0.3	1.116	22.18	71.65	17.74
0.5	1.093	22.57	77.13	19.02
0.8	1.130	22.17	71.82	18.00
1.0	1.108	22.24	71.35	17.59

**Table S3.** Photovoltaic performance of TM6-coated PSCs with different concentrations.

<i>c</i> /mg cm <sup>-3</sup>	<i>V</i> <sub>oc</sub> /V	<i>J</i> <sub>sc</sub> /mA cm <sup>-2</sup>	FF/%	PCE/%
0	1.026	22.14	75.78	17.22
0.3	1.128	22.13	72.35	18.07
0.5	1.118	22.96	75.59	19.40
0.8	1.107	22.98	75.26	19.13
1.0	1.110	23.09	71.15	18.23

**Table S4.** Photovoltaic performance of PSCs with different HTLs.

HTL	$V_{oc}/V$	$J_{sc}/mA\ cm^{-2}$	FF/%	PCE/%
Undoped Spiro-OMeTAD	0.961	20.55	32.82	6.48
Doped Spiro-OMeTAD	1.046	22.12	72.70	16.81
Undoped TM5	1.053	22.05	59.18	13.74
Doped-TM5	1.029	21.72	59.56	13.31
Undoped TM6	1.098	21.79	63.87	15.29
Doped-TM6	1.101	21.58	65.97	15.67

**Table S5.** The SCLC parameters of the TM6-based devices measured under dark condition.

$c/mg\ cm^{-3}$	$V_{TFL}/V$	$N_t/cm^{-3}$
0.0	0.708	$2.78 \times 10^{15}$
0.3	0.320	$1.26 \times 10^{15}$
0.5	0.127	$4.99 \times 10^{14}$
1.0	0.122	$4.79 \times 10^{14}$
2.0	0.122	$4.79 \times 10^{14}$

**Table S6.** The carrier lifetimes and corresponding parameters of perovskite films.

Films	$A_1$	$\tau_1/ns$	$A_2$	$\tau_2/ns$	$\tau_{ave}/ns$
Perovskite	1.21%	72	98.79%	271	269
Perovskite/TM5	2.31%	28	97.68%	179	176
Perovskite/TM6	6.08%	24	93.92%	160	152
Perovskite/HTL	6.73%	19	93.27%	59	56
Perovskite/TM5/HTL	6.92%	7	93.08%	23	22
Perovskite/TM6/HTL	7.21%	5	92.79%	14	17

**Table S7.** Parameters for Mott-Schottky plots.

PSC	$V_{bi}$ (V)	Slope of $C^{-2}$ vs. $V$ ( $F^{-2}\ V^{-1}$ )	$N_d$ ( $cm^{-3}$ )
Control	0.87	$-7.58 \times 10^{13}$	$7.19 \times 10^{18}$
TM5-coated	0.96	$-8.98 \times 10^{13}$	$6.13 \times 10^{18}$
TM6-coated	1.00	$-9.14 \times 10^{13}$	$5.96 \times 10^{18}$

**References:**

1. G. Yang, C. Chen, F. Yao, Z. Chen, Q. Zhang, X. Zheng, J. Ma, H. Lei, P. Qin, L. Xiong, W. Ke, G. Li, Y. Yan and G. Fang, *Adv. Mater.*, 2018, **30**, 1706023.
2. Q. F. Dong, Y. J. Fang, Y. C. Shao, P. Mulligan, J. Qiu, L. Cao and J. S. Huang, *Science*, 2015, **347**, 967-970.